Normalizing the behavior of unsaturated granular pavement materials

ASCE paper GT/2003/023443

by Andrew C. Heath[1], Juan M. Pestana (Member, ASCE)[2], John T. Harvey (Member, ASCE)[3] and Manuel O. Bejerano (Associate Member, ASCE)[4]

Abstract

One of the important components of a flexible pavement structure is granular material layers. Unsaturated granular pavement materials (UGPMs) in these layers influence stresses and strains throughout the pavement structure, and have a large effect on asphalt concrete fatigue and pavement rutting (two of the primary failure mechanisms for flexible pavements.) The behavior of UGPMs is dependent on water content, but this effect has been traditionally difficult to quantify using either empirical or mechanistic methods.

This paper presents a practical mechanistic framework for determining the behavior of UGPMs within the range of water contents, densities, and stress states likely to be encountered under field conditions. Both soil suction and generated pore pressures are determined and compared to confinement under typical field loading conditions. The framework utilizes a simple soil suction model that has three density-independent parameters, and can be determined using conventional triaxial equipment that is available in many pavement engineering laboratories.

[1]Lecturer, Department of Architecture and Civil Engineering, University of Bath, Bath, BA2 7AY, UK.

[2]Associate Professor, Department of Civil and Environmental Engineering, University of California, Berkeley, CA, 94720.

[3]Associate Professor, Department of Civil Engineering, University of California, Davis, CA, 95616.

[4]Associate Research Engineer, Pavement Research Center, University of California, 1353 S 46th St., Richmond, CA, 94804.

Key Words: Unsaturated soils, Granular materials, Pavements, Soil suction

INTRODUCTION

Soil effective stress in the presence of more than one pore fluid (typically water or air) is more complicated than the situation where only one pore fluid is present. The behavior of soils under completely dry or completely saturated conditions is fairly well understood, but the understanding of the unsaturated case is not as advanced. The pore fluid in granular pavement materials is normally a two phase system consisting of both water and air, while other geotechnical engineering applications could include other gases or liquids.

Water content has been shown to have a large effect on granular pavement material response, but attempts to quantify this effect have mainly been through empirical methods (e.g. Theyse (2000)). This paper presents a mechanistic framework for normalizing the response of unsaturated granular pavement materials (UGPMs). This framework can be used in conjunction with an effective stress constitutive model to determine the response of UGPMs within a range of water contents under typical field loading conditions. Although the procedure is aimed specifically at UGPMs, the framework can be extended to other geotechnical applications within a certain set of constraints which are detailed later in the paper. The framework is validated using laboratory test data from a typical California aggregate base (AB) material, and additional validation using an aggregate base material from recycled crushed concrete is presented in Heath et al. (2002).

PAVEMENT SATURATION CONDITIONS

The level of soil saturation (S_w) can be defined as:

$$S_w = \frac{w\,G_s}{e} \quad : \quad 0 \leq S_w \leq 1 \tag{1}$$

where e is the void ratio, w is the gravimetric water content and G_s is the ratio of the soil particle density to water density. Gravimetric water contents in UGPMs are usually below 10% by mass of dry material, and dry soil unit weights ($\gamma_{s,d}$) are typically between 2.0 and 2.3 (dry density of between 2.0 and 2.3 times that of water). The water saturation at different densities and water contents is illustrated in Figure 1, based on a G_s of 2.72. Included with the saturation curves is a typical compaction curve for the AB material used for this research with compaction according to the modified method (ASTM, 2000).

EFFECTIVE STRESS FOR UNSATURATED SOILS

The behavior of unsaturated soils is more complex than completely saturated or completely dry soils, because of the difference in compressibility of the pore fluid phases, and because of matric suction caused by water surface tension on the curved pore air / pore water interface. The pore air pressure can be calculated using the pore fluid compressibility, and the pore water pressure calculated using the matric suction and the pore air pressure. This approach requires an additive effective stress relation originally proposed by Bishop (1959), and includes the net normal stress $(\sigma_{ij} - \delta_{ij} u_a)$ and matric suction $(u_a - u_w)$ as stress state parameters:

$$\begin{aligned} \sigma'_{ij} &= (\sigma_{ij} - \delta_{ij} u_a) + \delta_{ij} \chi_w (u_a - u_w) \\ &= (\sigma_{ij} - \delta_{ij} u_a) + \delta_{ij} p_{suc} \end{aligned} \tag{2}$$

where σ'_{ij} is an effective stress tensor component, σ_{ij} is a total stress tensor component, δ_{ij} is the Kronecker delta function ($\delta_{ij} = 1$ if $i = j$, and $\delta_{ij} = 0$ if $i \neq j$), u_a and u_w are the pore air and pore water pressures, χ_w is the Bishop parameter, and $p_{suc} = \chi_w (u_a - u_w)$ is the effective suction confinement. The form of this equation is such that only normal stresses are influenced by pore pressures, and the pore fluid is unable to support shear.

Equation 2 is used by Khalili and Khabbaz (1998), Zienkiewicz et al. (1999) and Gallipoli et al. (2003), but other researchers (e.g. Muraleetharan and Wei (1999) and Fredlund and Rahardjo (1993)) have indicated that Equation 2 is valid only under certain conditions. This is because χ_w depends primarily on the saturation, but also on the material, compaction procedures and stress path. This parameter has the same limits as saturation ($0 \leq \chi_w \leq 1$) and is equal to the saturation for the completely dry and completely saturated cases. The relationship between S_w and χ_w for a number of materials is illustrated in Figure 2 (Blight, 1961; Donald, 1961). There is a lack of data at very low saturation and the form of the relation in this range is not well understood, but this is of little consequence to UGPM modelling as these low saturation levels are unlikely to be encountered under field conditions. In order to obtain p_{suc} for an unsaturated soil (Equation 2), χ_w from Figure 2 must be multiplied with $(u_a - u_w)$, ensuring $p_{suc} \leq (u_a - u_w)$.

SOIL SUCTION

The matric suction is the component of total soil suction equal to the difference in air and water pressure, and the relation between matric suction and water content is often referred to as the soil-water characteristic curve. Although, there is hysteresis in the soil-water characteristic curve between wetting and drying cycles (e.g. Gonzalez and Adams (1980), Wheeler et al. (2003)) this is often ignored in geotechnical engineering, an approach which may not be acceptable for pavement engineering applications where near-surface confining stresses are low. An example of a soil-water characteristic curve for a fine sand, showing the hysteresis between wetting and drying cycles is illustrated in Figure 3.

The shape of the soil-water characteristic curve is highly dependent on the material type and Figure 4 shows typical curves for different soils (Vanapalli et al., 1999). There is considerable variation in the soil-water characteristic curve resulting from different measurement methods, different sampling techniques and inherent variability between samples (Ridley et al., 2003; Vanapalli et al., 1999), but this variation is seldom considered by researchers and practitioners. Fine-grained soils (such as clays) generally have higher matric suction than coarser-grained soil (Figure 4), and loose clays can undergo large volumetric changes as a result of changes in suction (water content). Because UGPMs do not have a large fines content and are generally well compacted, this usually results in very small volumetric strains from changes in water content.

A number of equations have been proposed to describe the soil-water characteristic curve. An example is the empirical equation proposed by van Genuchten (1980) that requires only three parameters, and can be easily re-formulated to give a closed form solution for either water content as a function of suction, or suction as a function of water content, and is presented here with matric suction as a function of water content:

$$(u_a - u_w)/p_{at} = v_1 \ ({S_w}^{v_2} - 1)^{v_3} \tag{3}$$

where p_{at} is atmospheric pressure and v_{1-3} are regression constants. This equation has certain limitations, with the major concern related to overprediction of suction as saturation approaches zero. It is, however, considered a practical model for determining the mechanical behavior of coarse grained UGPMs within the range of suction values experienced under field conditions. This model is not recommended for fine-grained cohesive soils and the remainder of this paper does not consider suction of over 100 atm.

Soil suction in compacted soils has been shown to be largely independent of material density in the lower saturation range (Krahn and Fredlund, 1972; Romero et al., 2003), with the saturation level below which this behavior occurs dependent on the soil type and density. The density independence of suction is shown in Figure 5 which illustrates total and matric suction as a function of w for a low plasticity glacial till (Plasticity Index = 16.9), compacted to different dry densities ($\gamma_{s,d}$). While the soil suction is independent of density in the saturation range shown on the figure, this is not the case at high saturation levels as denser samples will become completely saturated (suction $\rightarrow$ 0) at lower water contents than is the case with looser samples.

The relation proposed by van Genuchten (1980) (Equation 3) and most other equations describing the soil-water characteristic curve are based on saturation rather than on water content. While this ensures $(u_a - u_w) \rightarrow 0$ as $S_w \rightarrow 1$, the dependence on saturation results in a dependence on density at lower saturation, and the behavior in Figure 5 cannot be effectively modelled without the use of different model parameters for different densities. This is a limitation of many existing models, and a new density-independent form of the van Genuchten (1980) relation is therefore proposed.

PORE FLUID COMPRESSIBILITY

The pore fluid in an UGPM is usually a mix of air and water, and the compressibility of this mixture influences generated pore pressures. While water is often considered incompressible in geotechnical engineering this is not strictly correct. However, the compressibility of water is very low compared to air in the range of pressures in pavement engineering applications (air pressure is usually equal to atmospheric pressure). If the pore fluid drains freely (drained loading) any generated pore pressures will dissipate. For undrained conditions, the change in pore air pressure can be calculated using the change in pore air volume and Boyle's law for an ideal gas. Increasing the air pressure will increase the mass of air dissolved in the water and this can be calculated using Henry's law. Conventional traffic loading of UGPMs results in small volumetric deformations during a single load cycle, and it is therefore possible to use a simplified approach where water is considered incompressible relative to air. For undrained loading of an unsaturated soil at constant temperature Boyle's law can be written as:

$$u_a = (u_{ao} + p_{at}) \frac{e_o + wG_s(h-1)}{e + wG_s(h-1)} - p_{at} \tag{4}$$

where u_{ao} and e_o are the pore air pressure and void ratio at the start of loading, and h is the volumetric coefficient of solubility (approximately 0.02 at 20°C (Moran and Shapiro, 1996)). For undrained loading, u_a from Equation 4 can be substituted into Equation 2 to determine the effective stress. Volumetric strains in soils (changes in e) depend on effective stress, and Equations 2 and 4 shows that effective stress, in turn, depends on volumetric strains. As a result, it is necessary to use an interative solution to determine both volumetric strains and effective stress during undrained loading of unsaturated soils.

NORMALIZING THE RESPONSE OF UGPMS

Normalizing the strength and stiffness of UGPMs enables the behavior over a range of water contents to be determined. This effective stress can be included with an effective stress constitutive model to predict behavior of UGPMs under field loading conditions. In order to normalize the response of the material, the Bishop's effective stress relationship for unsaturated soils (Equation 2) is used.

Normalizing matric suction

Most pavement engineering laboratories do not have the equipment to directly measure the soil-water characteristic curve and even if this curve is known, the effective suction confinement (p_{suc}) and not the matric suction is what is required to determine effective stress in an unsaturated soil. Furthermore, the hysteresis in the soil-water characteristic curve (Figure 3) and the inherent variability in suction between different samples (e.g. Vanapalli et al. (1999); Ridley et al. (2003)) limit the direct use of the soil-water characteristic curve to determine effective stresses in UGPMs where near-surface confining stresses are low. Because all these factors increase uncertainty in effective stress prediction, a procedure to back-calculate p_{suc} from simple laboratory shear tests is proposed. The relationship between water content and p_{suc} can then be included with an effective stress constitutive model to predict the behavior of UGPMs at different water contents, stress states and loading conditions.

Khalili and Khabbaz (1998) summarized laboratory studies on a number of different materials and concluded the relation between χ_w and $(u_a - u_w)$ is linear in log-log space at suction levels above the air-entry value. If this relation is combined with the van Genuchten (1980) equation for the soil-water characteristic

curve (Equation 3), the relation between w and p_{suc} (or S_w and p_{suc}) will also be linear where suction is above the air-entry value. The following equation is therefore a combination of the empirical equations of Bishop (1959), van Genuchten (1980), and Khalili and Khabbaz (1998):

$$\frac{p_{suc}}{p_{at}} = \frac{wG_s}{e}\, n_1 \left(\frac{1}{(wG_s)^{n_2}} - \frac{1}{e^{n_2}} \right)^{n_3/n_2} \tag{5}$$

where n_{1-3} are density-independent regression parameters. Equation 5 predicts a linear relation in log-log space at intermediate and low saturation levels, and includes a smooth transition to $p_{suc} = 0$ at full saturation. Data for the Bishop (1959) model (Equation 2) was obtained by multiplying the matric suction with the χ_w data for the silt materials in Figures 4 and 2, and this test data is compared to Equation 5 in Figure 6. As shown, the proposed density-independent model (Equation 5) effectively represents the laboratory data, and confirms the linear relation between w (S_w) and p_{suc} at intermediate and low saturation levels.

Equation 5 does not require $(u_a - u_w)$ or χ_w, but instead calculates the combined effect. It is not possible to directly separate these two parameters, but an approximate soil-water characteristic curve can be determined by assuming $\chi_w = S_w$:

$$\frac{(u_a - u_w)}{p_{at}} \approx n_1 \left(\frac{1}{(wG_s)^{n_2}} - \frac{1}{e^{n_2}} \right)^{n_3/n_2} \tag{6}$$

The approximate equation above is a density-independent form of the van Genuchten (1980) relation, and the assumption of $\chi_w = S_w$ has the additional theoretical benefit of ensuring the energy balance at microscopic and macroscopic levels is consistent (Zienkiewicz et al., 1999). Equation 6 describes a family of approximate soil-water characteristic curves for different densities (different values of e), as illustrated in Figure 7. There was insufficient matric suction data presented by Krahn and Fredlund (1972) to compare the model to test data, and the total suction data from Figure 5 is therefore presented. Because there is no data on the transition to full saturation, the model parameters defining the transition were estimated and the curves are shown to asymptote to the saturation water content (w_{sat}). Difficulties in obtaining constant-volume suction measurements has resulted in a lack of good quality data on this behavior, and has prevented more accurate estimates of the transition to full saturation.

Equation 6 is characterized by a limiting suction curve (LSC) that describes the density independent matric suction in the mid to low saturation ranges, but still ensures the suction tends to zero at full satura-

tion. This overcomes the density dependence of previous models (e.g. Equation 3 (van Genuchten, 1980)), enabling the behavior at different water contents and densities to be quantified without requiring new model parameters. As with the van Genuchten (1980) model, if the density and water content parameters are known, only three parameters (n_{1-3}) are required to determine the effective suction confinement over the range of densities and moisture conditions likely to be encountered in UGPMs. The suction tends to zero as $wG_s \rightarrow e$ (full saturation), and to the unique LSC as w decreases. The effect of n_{1-3} is best visualized in log-log space with the water content converted from a percentage and multiplied with G_s. As shown in Figure 8, the parameter n_1 describes the intercept of the LSC at wG_s=1, and varying this parameter shifts the curve left or right. The parameter n_2 controls the transition to full saturation with Equation 6 predicting a bi-linear relation (sharp transition) as $n_2 \rightarrow \infty$. The parameter n_3 represents the slope of the LSC in log-log space with the value of n_3 equal to the ratio of log scale changes in matric suction to log scale changes in wG_s. As mentioned earlier, Equation 5 is a simplified form of the Bishop (1959) and van Genuchten (1980) equations and includes the combined effect of χ_w and $(u_a - u_w)$. It therefore has the same limitations of these equations, and is not recommended for use with fine-grained soils where large suctions or where large volumetric strains are expected.

Back-calculating p_{suc} from laboratory shear test data does have a number of advantages over the approach of considering $(u_a - u_w)$ and χ_w independently. If the laboratory tests are performed at similar conditions to those expected in the field, the back-calculation procedure will minimize the effect of hysteresis in the soil-water characteristic curve, minimize the effect of the stress path dependence of χ_w, and enable the inherent variability in suction measurements to be included. In addition, a standard triaxial test apparatus is the only test equipment required.

Generated pore pressures

No pore air pressures will be generated during drained loading, and the pore air pressures generated during undrained loading can be calculated using Equation 4. This requires measurement of volumetric strains, a procedure that is complicated if monotonic shearing results in volume changes along a single failure plane. Although pore air pressures generated during monotonic shearing of UGPMs are likely to be low, it is

recommended that laboratory testing be performed under drained conditions to simplify back-calculation procedures.

LABORATORY TESTING

In order to normalize the unsaturated response, it is necessary to prepare samples where the only difference is the variation in moisture content and density. This presents some difficulty as the easiest method of preparing samples at different water contents is to compact them at the required water content. The difference in soil fabric (dispersed or flocculated) between cohesive materials compacted wet and dry of the optimum water content (w_{opt}) has been well documented (e.g. Seed et al. (1962)). Although the aggregate base (AB) material used for this research is non-plastic, permeability tests, monotonic triaxial tests and dynamic triaxial tests indicated strong evidence of fabric differences for samples compacted wet or dry of w_{opt} (Russo, 2000; Heath, 2002). An example of this behaviour is shown in Figure 9 where small changes in w around w_{opt} resulted in large changes in strength and stiffness during monotonic triaxial testing (Heath, 2002). The AB samples with a dispersed fabric were therefore taken as one sample group and the samples with a flocculated fabric were taken as another.

Monotonic shear

The Mohr-Coulomb failure criteria is probably the most popular simple method of determining the peak shear strength of soils:

$$\tau_{ff} = c' + \sigma'_n \tan\phi' \tag{7}$$

where τ_{ff} is the shear strength on the failure plane, c' is the effective cohesion, σ'_n is the effective stress normal to the shear plane, and ϕ' is the effective friction angle. The Mohr-Coulomb criteria is not an accurate representation of peak shear strength for a number of reasons. One of these is that many newly deposited soils can be considered to have no true cohesion (i.e. $c' = 0$) which is in line with Coulomb's original work (Heyman, 1972), and that of many other researchers (e.g. Schofield (1998); Pestana and Whittle (1999)). Apparent cohesion can come from a number of sources, including matric suction in unsaturated soils and slow pore water flow in saturated clays. A second reason for the inaccuracy of the Mohr-Coulomb criteria

is that experimental evidence has shown ϕ' is not constant for dense granular materials at low confining stresses and the following equation fits triaxial shear test data on granular soils (Duncan et al., 1980):

$$\phi' = \phi'_o - \Delta\phi' \log\left(\frac{\sigma'_3}{p_{at}}\right) \tag{8}$$

where ϕ'_o is the effective friction angle at an applied confining pressure equal to atmospheric pressure, $\Delta\phi'$ is the change in effective friction angle with confining stress, and σ'_3 is the minor principal effective stress (effective confining stress in a triaxial compression test). The monotonic shear testing for this research was performed under drained conditions and no significant pore air pressures were therefore generated during loading. As a result, σ'_3 in Equation 8 is taken as the sum of the total confining stress (σ_3) and p_{suc} from Equation 5. This requires five parameters (ϕ'_o, $\Delta\phi'$ and n_{1-3}) to determine the monotonic shear strength of an unsaturated soil at any given density and soil fabric. As the matric suction (Equation 6) is independent of density but the friction angle depends on sample density and soil fabric, two parameters (ϕ'_o and $\Delta\phi'$) are required at each additional density or soil fabric.

Resilient response

Dynamic testing to determine the resilient properties of UGPMs can be performed using the Strategic Highways Research Program (SHRP) P46 protocol (FHWA, 1996). This test is performed using a triaxial apparatus and involves applying different amplitude haversine shaped deviatoric pulses at a specified range of confining stresses. The applied deviatoric stress and resultant elastic deformations are measured, enabling calculation of a resilient modulus. Because loading is primarily in the elastic range and there is a short (100 ms) loading time and longer (900 ms) rest time between pulses, loading was assumed to be undrained during the pulse application, but drained (pore pressures allowed to dissipate) between successive loads. A description of the apparatus used for this testing is provided in Bejarano et al. (2002). It is not currently possible to accurately measure generated pore air pressures during the 100 ms load pulses in a P46 test, and the generated pore pressures were therefore calculated using Equation 4 and used to determine the effective stress. The Uzan (1985) model for the resilient modulus of UGPMs can be written in a dimensionless form:

$$\frac{M_r}{p_{at}} = k_1 \left(\frac{p'}{p_{at}}\right)^{k_2} \left(\frac{q}{p_{at}}\right)^{k_3} \tag{9}$$

where M_r is the resilient modulus, $p' = (\sigma'_1 + \sigma'_2 + \sigma'_3)/3$ is the mean effective stress, $q = \sigma_1 - \sigma_3$ is the deviatoric stress, and k_{1-3} are regression constants. There are other simple bulk stress models that ignore the deviatoric component (e.g. Dehlen and Monismith (1970); Hicks and Monismith (1971)), but these do not provide as accurate a description of resilient behavior. For undrained loading during a P46 test, the mean effective stress is calculated using the applied total stress, effective suction confinement (Equation 5) and generated pore air pressures (Equation 4):

$$p' = \frac{\sigma_1 + \sigma_2 + \sigma_3}{3} + p_{suc} - u_a \tag{10}$$

Each P46 test has 15 blocks with different confining and deviatoric stresses, and the model in Equation 9 has only four unknown parameters (k_{1-3} and p_{suc}). If the three suction parameters for Equation 5 are already known from monotonic shear tests, one P46 test is required to determine the response of a material for a given density and soil fabric. If the suction parameters are not known, it is possible to use P46 tests at a minimum of three water contents to back-calculate n_{1-3} to determine the effect of water content on resilient response. Because of the variability in small strain stiffness measurements on UGPMs (Chan and Brown, 1991; Bejarano et al., 2002), the use of monotonic shear data is preferred for the calculation of soil suction for stiff, brittle soils.

EXPERIMENTAL VALIDATION

The testing preformed as part of this research is summarized in Bejarano et al. (2002) and Heath (2002), and only selected results are used for validation.

Monotonic shear

Conventional total stress analysis using the Mohr-Coulomb failure criteria (Equation 7) assumes some apparent cohesion (c). Because of the small range in confining stress, the total friction angle ϕ was assumed constant and total stress failure envelopes for the AB material are illustrated in Figure 10. The results are illustrated for two void ratios (densities) of $e = 0.241$ and $e = 0.179$ (95% and 100% of the maximum dry density according to the modified compaction method (ASTM, 2000)). The samples in Figure 10 all have a flocculated fabric, and are grouped according to a target w of 3% and 5% for $e = 0.241$, and a target w

of 5% for $e = 0.179$. To enable easy visualization of the data, the points in the figure are the failure points (τ_{ff} and σ_n) calculated using the failure envelopes shown. These failure points indicate the position on the Mohr circle where the circle has the same gradient as the failure surface. If there is no experimental error, these failure points will be the point where the failure surface is tangent to the Mohr's circle.

In order to calculate the effective stress under unsaturated conditions, a least squares regression was performed using the peak strengths and water contents from the monotonic triaxial tests. This enabled the three suction parameters for the material (n_{1-3}) and the friction angle (ϕ'_o and $\Delta\phi'$) at each density and soil fabric to be determined. The approximate back-calculated soil-water characteristic curve (Equation 6) for the material is illustrated in Figure 11, which also contains the three suction model parameters (n_{1-3}) as well as the two friction parameters at each density and soil fabric (ϕ'_o and $\Delta\phi'$). As shown, the peak friction angle increases as the density increases, and as the fabric moves from a dispersed to flocculated structure.

The approximate soil-water characteristic curve is slightly different from the examples in Figure 4, mainly because the void ratio of compacted UGPMs is much lower than that of most other soils, resulting in full saturation (matric suction tends to zero) at lower water contents than for most soils. The effective suction confinement is affected by sample density, as illustrated in Figure 12. In this figure the curves are plotted as a function of saturation on a log-log scale to allow easier comparison of the relative shapes. As shown, p_{suc} for the materials is large compared to the applied confinement during a P46 test (maximum of $\sigma_3/p_{at} = 1.4$), indicating the suction is supplying a major portion of the effective confinement during the test.

The effective confinement for the monotonic triaxial testing was increased by adding p_{suc} (Equation 5) to the applied confining stress, and calculating new effective stress failure envelopes. This is illustrated in Figure 13 for the same AB samples shown in Figure 10. The difference in the total stress envelopes in Figure 10 (include c) and the effective stress envelopes in Figure 13 (that include suction and c=0) is evident. The envelopes in Figure 13 go through the origin because the framework assumes there is no true cohesion in uncemented materials, a property noted by numerous other researchers (e.g. Schofield (1998); Pestana and Whittle (1999)). The test data on this and other UGPMs indicates this assumption is reasonable (Heath et al., 2002).

If the peak shear strength envelopes at three densities and three moisture contents are required, signifi-

cantly less tests are required for the framework outlined here than for a conventional total stress approach. If the total stress approach is used with a non-linear failure envelope, the minimum number of tests required (assuming no experimental variation) is 3 shear parameters × 3 densities × 3 moisture contents = 27 samples. Slight variations in compaction moisture content could affect results and some tests may have to be repeated. If the normalized approach is used to back-calculate the shear strength and suction parameters, and there is no effect of soil fabric, the number of tests decreases to 2 shear parameters × 3 densities + 3 suction parameters = 9 samples. If there is evidence of soil fabric, this will increase to 2 shear parameters × 3 densities × 2 fabrics + 3 suction parameters = 15 samples, still significantly less than that required for the total stress approach. In addition, any variations in sample moisture content can be easily accommodated without having to repeat tests.

The normalized approach provides a mechanistic framework for determining the response at moisture contents other than those used in the testing, and provides a framework for other aspects of material behavior, such as for determining the resilient response.

Resilient response

As the volumetric behavior during the P46 dynamic testing was monitored using the on-sample instrumentation, it was possible to back-predict the pore air pressure (u_a) using Equation 4. Assuming a fully saturated soil is incompressible, it is possible to calculate a theoretical maximum increase in pore pressure that is equal to the increase in mean total stress (p) during each load cycle. The theoretical maximum generated pore pressure and a summary of u_a and p_{suc} as a function of saturation are illustrated in Figure 14. Because u_a changes through the different P46 test blocks while p_{suc} remains constant, only the peak value of u_a from all the test blocks is given. As expected, the samples with a higher S_w have higher generated pore pressures, although these are still very low compared to the effective confinement from soil suction, p_{suc} (less than three orders of magnitude (0.1%) in all samples tested). As the samples approach full saturation, the pore pressures will increase and the suction will decrease, leading to the softer, weaker samples noted during testing (e.g. Theyse (2000)). Because u_a is much smaller than p_{suc} at medium to low saturation, it is possible to ignore generated pore pressures for many practical pavement engineering purposes, which

simplifies computation by eliminating the need for an iterative solution to determine effective stress under unsaturated conditions.

As validation for the framework under different loading conditions, predictions using the Uzan model (Equation 9) are compared with the measured resilient modulus for samples with $w \approx 3\%$ and $w \approx 5\%$ in Figure 15. For the first data set, a total stress approach was used (soil suction was ignored) and the total stress Uzan model parameters were determined using a least squares regression on all the data, regardless of water content. For the second data set, p_{suc} was included using the suction model parameters calculated from the monotonic triaxial test data (Figure 11), and performing a new least squares analysis to obtain effective stress Uzan model parameters.

If suction is ignored, the samples cannot be considered to come from the same sample group and the coefficient of correlation between the measured resilient modulus and model predictions is only 0.25. The inclusion of matric suction produces a much improved estimate of response, and the coefficient of correlation increases to 0.69 and appears to be limited by the variability in resilient modulus measurements rather than the water content. If the effective suction confinement relation is known from monotonic testing, it is only necessary to perform one P46 test for each sample group (different density or soil fabric) to obtain the Uzan model parameters. Because of the variability in P46 test results, it is recommended that more than one test be performed.

LARGE STRAIN BEHAVIOR

While the procedure outlined above can be used to normalize the behavior of stiff, brittle UGPMs at low strains, Bishop's additive approach to unsaturated soil effective stress (Equation 2) is not applicable to large strain behavior. As UGPMs are unlikely to be sheared to large strains, this section is only included do demonstrate the limitations for softer, ductile materials where large strains are anticipated. Figure 16 shows the relationship between deviatoric stress (q) and axial strain (ε_a) during monotonic triaxial testing at different total confining stresses (σ_3) and water contents (w). If p_{suc} from Figure 12 is included, the two samples have similar effective confining stresses. As a result, the peak strengths and small strain stiffness are similar, but the post-peak behavior is very different with the drier sample (larger p_{suc} and smaller σ_3)

showing more brittle behavior than the wetter sample (smaller p_{suc} and larger σ_3). The AB samples are well compacted, dense and under low confinement, resulting in dilation along a single failure plane during large strain shearing. While this dilation will reduce the density and therefore p_{suc} along the failure plane (see Figure 12), this is not the primary cause of the difference in post-peak behavior.

The more brittle behavior of drier samples is more likely because the interface between the air and water is broken during shearing, leading to reduced suction confinement along the shear plane. This trend is also noted for other granular pavement materials (Heath et al., 2002) and could prevent the use of this framework for softer and more ductile materials, such as cohesive subgrade materials. As mentioned earlier, this is of little consequence to UGPMs as large strain shearing is unlikely to be encountered under normal field conditions.

SUMMARY OF PROCEDURE

The procedure for normalizing the behavior of UGPMs is summarized below:

- Perform a minimum of five drained monotonic triaxial shear tests on a soil with constant density and soil fabric. These tests should be performed over a range of water contents.
- Perform a minimum of two monotonic shear tests at each additional density or soil fabric.
- Use the Mohr-Coulomb failure criteria with $c' = 0$, and obtain the two shear parameters at each density and soil fabric, and the three unsaturated model parameters for the soil by performing a least squares (or other) regression analysis using the peak shear strengths.

The regression analysis requires the following equations:

$$\begin{aligned} \sin\phi' &= \frac{q_{max}}{2\sigma_3' + q_{max}} \\ \phi' &= \phi_o' - \Delta\phi' \log\left(\frac{\sigma_3'}{p_{at}}\right) \\ \sigma_3' &= \sigma_3 + p_{suc} \\ \frac{p_{suc}}{p_{at}} &= \frac{wG_s}{e}\, n_1 \left(\frac{1}{(wG_s)^{n_2}} - \frac{1}{e^{n_2}}\right)^{n_3/n_2} \end{aligned} \tag{11}$$

where σ_3 is the applied confining stress in the triaxial cell, q_{max} is the measured deviatoric stress at failure, ϕ'_o and $\Delta\phi'$ are the two shear regression parameters at each density and soil fabric, and n_{1-3} are the three suction regression parameters for the material. Once the material parameters have been obtained, the last line of Equation 11 can be used with other effective stress constitutive models for UGPMs.

CONCLUSIONS

This paper presents a mechanistic framework for determining the behaviour of unsaturated granular pavement materials. The effect of both generated pore pressures and soil suction are quantified and compared to the applied total stresses. For the material and saturation conditions tested, the soil matric suction is far larger (more than three orders of magnitude) than the generated pore pressures, and this suction can be greater than the applied confinement under typical field loading conditions.

The effective stress under small-strain unsaturated conditions can be back-calculated utilizing only triaxial test equipment that is available in many pavement engineering laboratories. The use of this framework significantly reduces the testing requirements when compared to conventional total stress approaches to granular pavement material modelling. The back-calculated effective stresses can be included in a three-dimensional finite element code with an effective stress constitutive model to determine the effect of soil moisture on pavement behavior.

The framework uses the Bishop (1959) relationship and a modified form of the van Genuchten (1980) suction model to determine effective stress. It therefore has the same limitations of these previous models, including the overprediction of effective confinement at high suctions (primarily in cohesive soils), and inaccurate suction predictions at large strains. It has, however, been validated for stiff, brittle, granular pavement materials at typical field densities, water contents and stress states.

APPENDIX I. REFERENCES

ASTM (2000). Test method for laboratory compaction characteristics of soil using modified effort (56,000 ft-lbf/ft^3(2,700 kN-m/m^3)). Test ASTM D1557-00, American Society for Testing and Materials, West Conshohocken, PA.

Bejarano, M. O., Heath, A. C., and Harvey, J. T. (2002). A low-cost high-performance alternative for controlling a servo-hydraulic system for triaxial resilient modulus apparatus. In *ASTM Symposium On Resilient Modulus Testing for Pavement Components*, Salt Lake City, UT.

Bishop, A. W. (1959). The principle of effective stress. *Tecknish Ukeblad*, 106(39):859–863.

Blight, G. E. (1961). *Strength and Consolidation Characteristics of Compacted Soils*. PhD thesis, University of London.

Chan, W. K. F. and Brown, S. F. (1991). Granular bases for heavily loaded pavements. Technical Report PR91019, University of Nottingham, Department of Civil Engineering, Nottingham, UK.

Dehlen, G. L. and Monismith, C. L. (1970). Effect of nonlinear material response on the behavior of pavements under traffic. *Highway Research Record*, 310:1–16.

Donald, I. B. (1961). *The Mechanical Properties of Saturated and Partly Saturated Soils with Special Reference to Negative Pore Water Pressures*. PhD thesis, University of London.

Duncan, J. M., Byrne, P., Wong, K. S., and Mabry, P. (1980). Strength, stress-strain and bulk modulus parameters for finite element analysis of stresses and movements in soil masses. Technical Report UCB/GT/80-01, University of California, Berkeley, CA.

FHWA (1996). LTPP materials characterization: Resilient modulus of unbound materials. Protocol P46, U.S. Department of Transportation, Federal Highway Administration. Research and Development, McLean, VA.

Fredlund, D. G. and Rahardjo, H. (1993). *Soil Mechanics for Unsaturated Soils*. Wiley and Sons, New York.

Gallipoli, D., Gens, A., Sharma, R., and Vaunat, J. (2003). An elasto-plastic model for unsaturated soil incorporating the effects of suction and degree of saturation on mechanical behaviour. *Géotechnique*, 53(1):123–135.

Gonzalez, P. A. and Adams, B. J. (1980). Mine tailings disposal: I. Laboratory characterization of tailings. Technical report, Dept of Civil Engineering, University of Toronto, Toronto, Canada.

Heath, A. C. (2002). *Modelling unsaturated granular pavement materials using bounding surface plasticity*. PhD thesis, University of California at Berkeley.

Heath, A. C., Pestana, J. M., Harvey, J. T., and Bejarano, M. O. (2002). Normalizing the response of unsaturated granular pavement materials. Draft technical report, University of California at Berkeley, Pavement Research Center, Berkeley, CA.

Heyman, J. (1972). *Coulomb's Memoir on Statics; An Essay in the History of Civil Engineering*. Cambridge University Press, Cambridge, U.K.

Hicks, R. G. and Monismith, C. L. (1971). Factors influencing the resilient response of granular materials. *Highway Research Record*, 345:15–31.

Khalili, N. and Khabbaz, M. H. (1998). A unique relationship for χ for the determination of the shear strength of unsaturated soils. *Géotechnique*, 48(5):681–687.

Krahn, J. and Fredlund, D. G. (1972). On total, matric and osmotic suction. *Soil Science*, 114(5):339–348.

Moran, M. J. and Shapiro, H. J. (1996). *Fundamentals of Engineering Thermodynamics*. Wiley and Sons, New York.

Muraleetharan, K. K. and Wei, C. (1999). Dynamic behaviour of unsaturated porous media: governing equations using the theory of mixtures with interfaces (TMI). *International Journal for Numerical and Analytical Methods in Geomechanics*, 23:1579–1608.

Pestana, J. M. and Whittle, A. J. (1999). Formulation of a unified constitutive model for clays and sands. *International Journal for Numerical and Analytical Methods in Geomechanics*, 23:1215–1243.

Ridley, A. M., Dineen, K., Burland, J. B., and R., V. P. (2003). Soil matrix suction: some examples of its measurement and application in geotechnical engineering. *Géotechnique*, 53(2):241–253.

Romero, E., Gens, A., and Lloret, A. (2003). Suction effects on a compacted clay under non-isothermal conditions. *Géotechnique*, 53(1):65–81.

Russo, M. A. (2000). Laboratory and field tests on aggregate base material for Caltrans accelerated pavement testing goal 5. Master's thesis, University of California at Berkeley.

Schofield, A. N. (1998). The "Mohr-Coulomb"error. *Mechanics and Geotechnique, LMS Ecole Polytechnique*, 23:19–27.

Seed, H. B., Chan, C. K., and Lee, C. E. (1962). Resilience characteristics of subgrade soils and their relation to fatigue failures in asphalt pavements. In *International Conference on the Structural Design of Asphalt Pavements*, pages 611–636, University of Michigan, Ann Arbor.

Theyse, H. L. (2000). The development of mechanistic-empirical permanent deformation design models for unbound pavement materials from laboratory and accelerated pavement test data. In *5th International Symposium on Unbound Aggregates in Roads, A. R. Dawson (Ed.)*, pages 285–293, Nottingham, U.K.

Uzan, J. (1985). Characterization of granular material. *Transportation Research Record*, 1022:52–59.

van Genuchten, M. T. (1980). A closed-form equation for predicting the hydraulic conductivity of unsaturated soils. *Soil Science Society of America Journal*, 44:892–898.

Vanapalli, S. K., Fredlund, D. G., and Pufahl, D. E. (1999). The influence of soil structure and stress history on the soil-water characteristics of a compacted till. *Géotechnique*, 49(2):143–159.

Wheeler, S. J., Sharma, R. J., and Buisson, M. S. R. (2003). Coupling hydraulic hysteresis and stress strain in unsaturated soils. *Géotechnique*, 53(1):41–54.

Zienkiewicz, O. C., Chan, A. H. C., Pastor, M., Schrefler, B. A., and Shiomi, T. (1999). *Computational Geomechanics with Special Reference to Earthquake Engineering*. Wiley and Sons, Chichester, U.K.

APPENDIX II. NOTATION

c	=	Total cohesion
c'	=	Effective cohesion
e	=	Void ratio
e_o	=	Void ratio at the start of loading
h	=	Volumetric coefficient of solubility
k_{1-3}	=	Regression constants for Uzan (1985) stiffness model
n_{1-3}	=	Regression parameters for new density independent suction model
p	=	Mean total stress
p'	=	Mean effective stress
p_{at}	=	Atmospheric pressure
p_{suc}	=	Effective suction confinement
q	=	Deviatoric stress
u_a	=	Pore air pressure
u_{ao}	=	Pore air pressure at the start of loading
$(u_a - u_w)$	=	Matric suction
u_w	=	Pore water pressure
v_{1-3}	=	Regression constants for van Genuchten (1980) suction model
w	=	Gravimetric water content
w_{opt}	=	Optimum water content for compaction
w_{sat}	=	Water content at 100% saturation
G_s	=	Ratio between soil particle and water unit weights
M_r	=	Resilient modulus
S_w	=	Soil saturation
$\gamma_{s,d}$	=	Dry soil unit weight
δ_{ij}	=	Kronecker delta function
σ_3	=	Minor principal total stress
σ_{ij}	=	Total stress tensor component
σ'_3	=	Minor principal effective stress
σ'_{ij}	=	Effective stress tensor component
σ'_n	=	Effective stress normal to the shear plane
τ_{ff}	=	Shear strength on the failure plane
ϕ	=	Total friction angle
ϕ'_o	=	Effective friction angle at an applied confining pressure of atmospheric pressure
ϕ'	=	Effective friction angle
χ_w	=	Bishop parameter
$\Delta\phi'$	=	Change in effective friction angle with confining stress

LIST OF FIGURES

Figure 1. Relationships between density, water content and saturation

Figure 2. Relation between S_w and χ_w for some materials (Blight, 1961; Donald, 1961)

Figure 3. Hysteresis in the soil-water characteristic curve (Gonzalez and Adams, 1980)

Figure 4. Soil-water characteristic curves for some materials (Vanapalli et al., 1999)

Figure 5. Soil suction at various densities for a low plasticity glacial till (Krahn and Fredlund, 1972)

Figure 6. Effective suction confinement as a function of saturation using the Bishop (1959) and proposed density -independent models

Figure 7. Density independent suction curve with total suction data from Krahn and Fredlund (1972)

Figure 8. Effect of parameters n_{1-3} on suction curve

Figure 9. Effect of soil fabric on monotonic triaxial stress and strain

Figure 10. Total stress failure envelopes for samples with flocculated structure

Figure 11. Approximate matric suction for AB material

Figure 12. Effective suction confinement at different void ratios

Figure 13. Effective stress failure envelopes for samples with flocculated structure

Figure 14. Ratio between u_a and p_{suc} during P46 testing

Figure 15. Comparison of measured and predicted resilient modulus

Figure 16. Difference in post peak shear behavior for samples with different w and σ_3

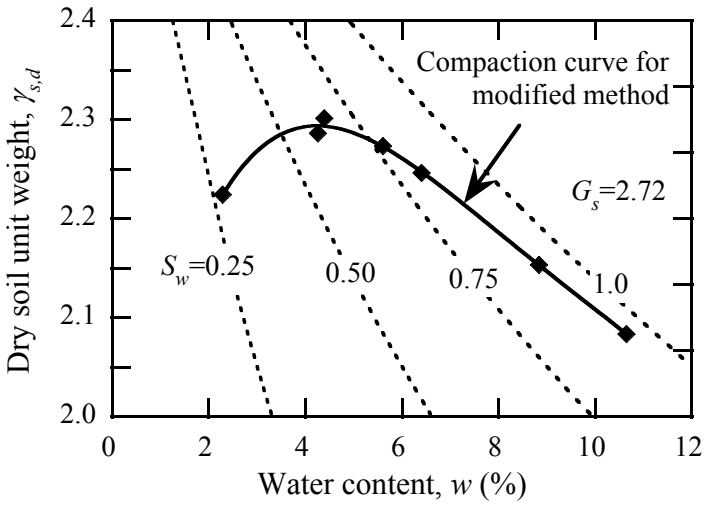

Figure 1: Relationships between density, water content and saturation

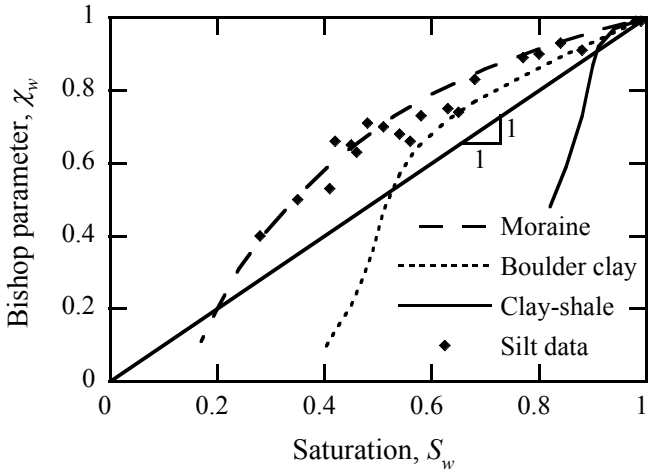

Figure 2: Relation between S_w and χ_w for some materials (Blight, 1961; Donald, 1961)

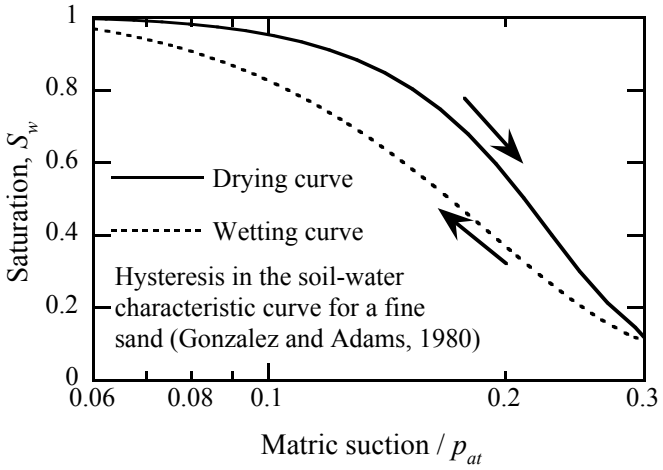

Figure 3: Hysteresis in the soil-water characteristic curve (Gonzalez and Adams, 1980)

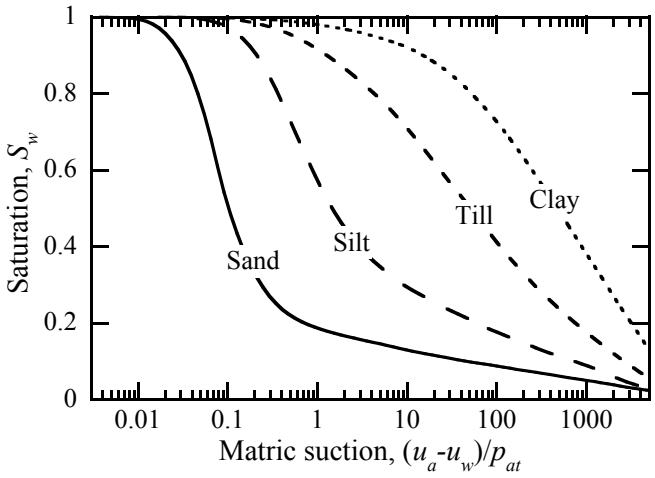

Figure 4: Soil-water characteristic curves for some materials (Vanapalli et al., 1999)

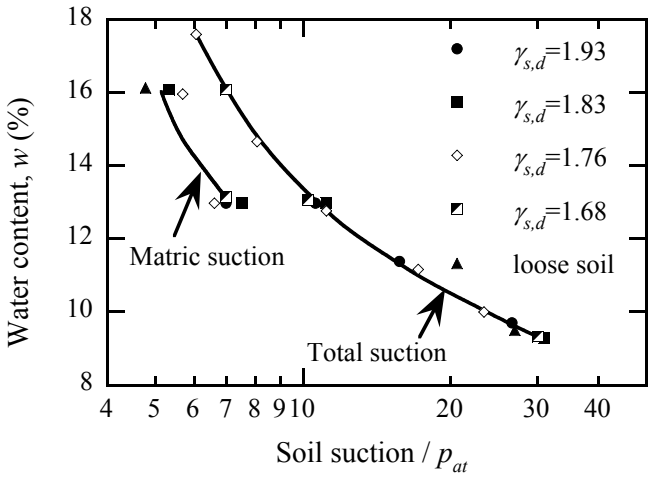

Figure 5: Soil suction at various densities for a low plasticity glacial till (Krahn and Fredlund, 1972)

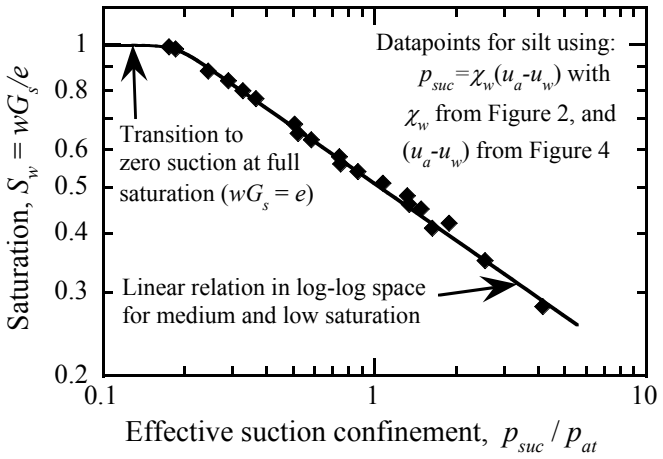

Figure 6: Effective suction confinement as a function of saturation using the Bishop (1959) and proposed density-independent models

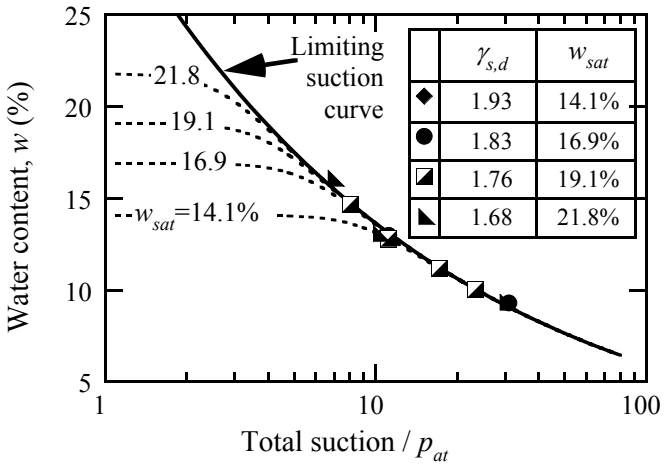

Figure 7: Density independent suction curve with total suction data from Krahn and Fredlund (1972)

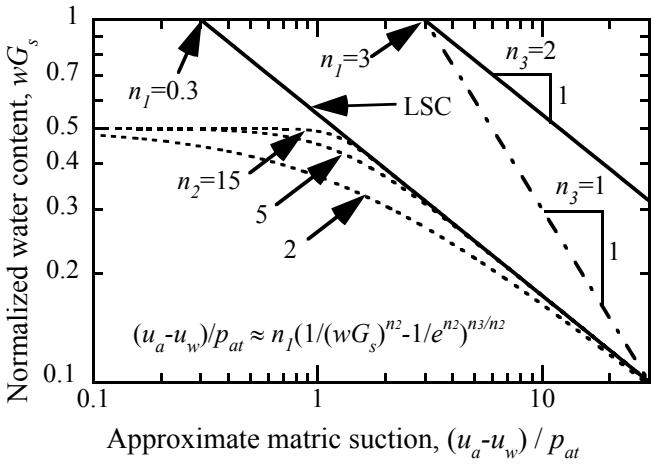

Figure 8: Effect of parameters n_{1-3} on suction curve

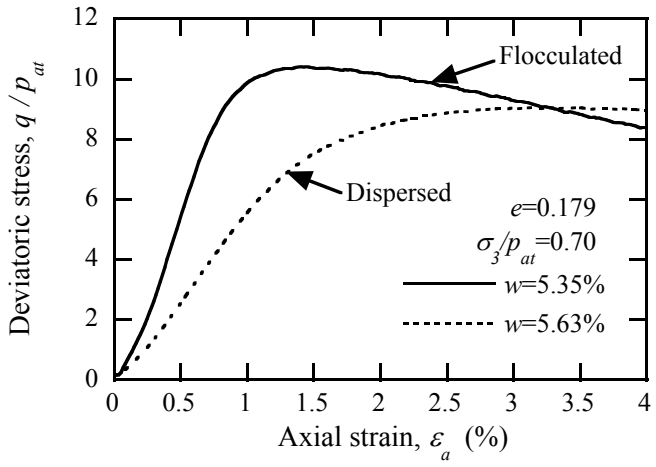

Figure 9: Effect of soil fabric on monotonic triaxial stress and strain

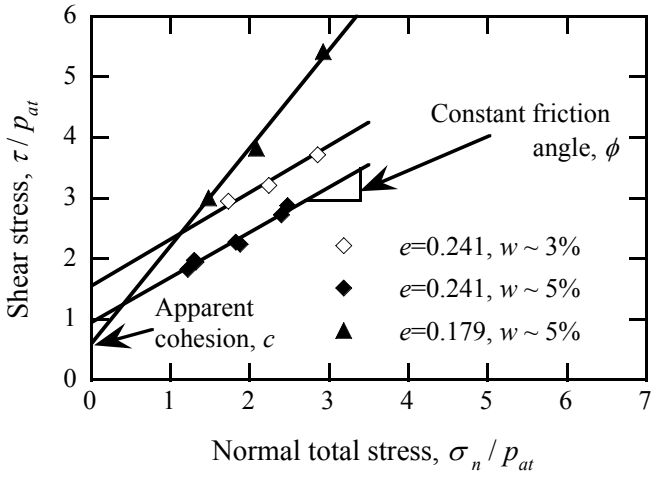

Figure 10: Total stress failure envelopes for samples with flocculated structure

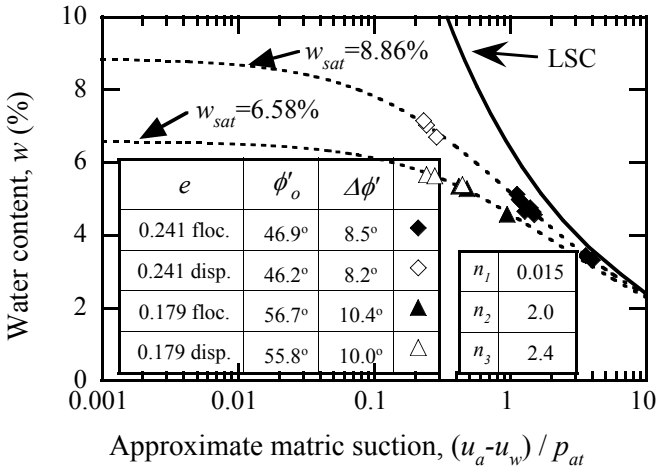

Figure 11: Approximate matric suction for AB material

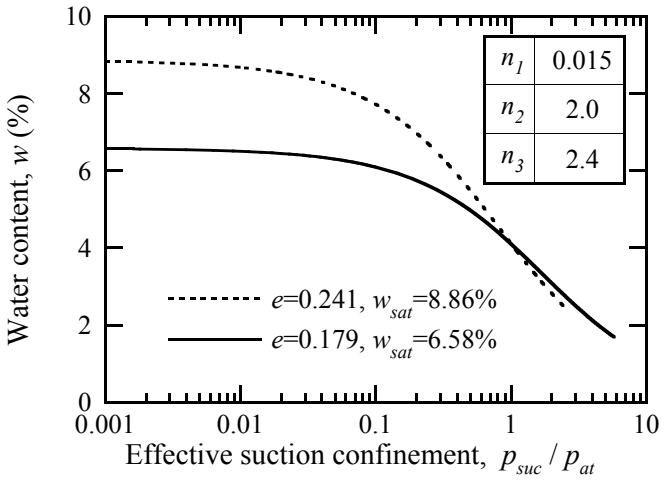

Figure 12: Effective suction confinement at different void ratios

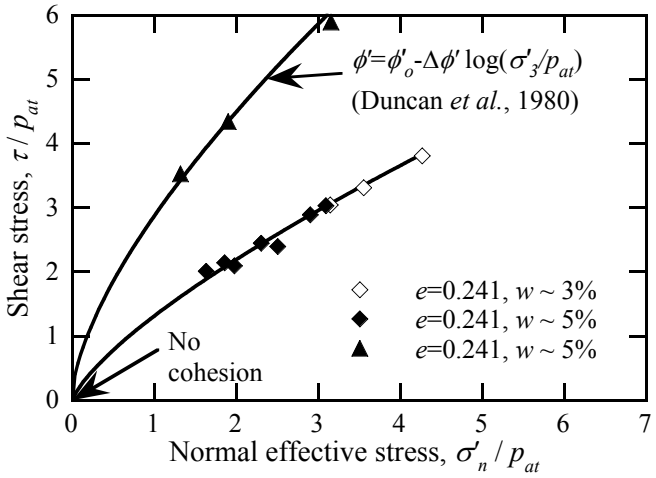

Figure 13: Effective stress failure envelopes for samples with flocculated structure

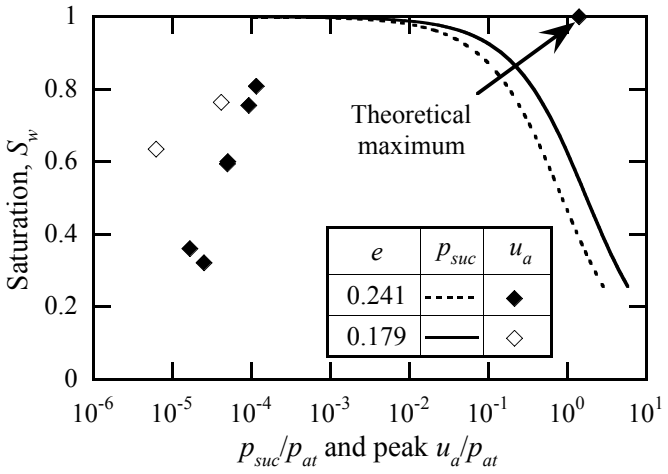

Figure 14: Ratio between u_a and p_{suc} during P46 testing

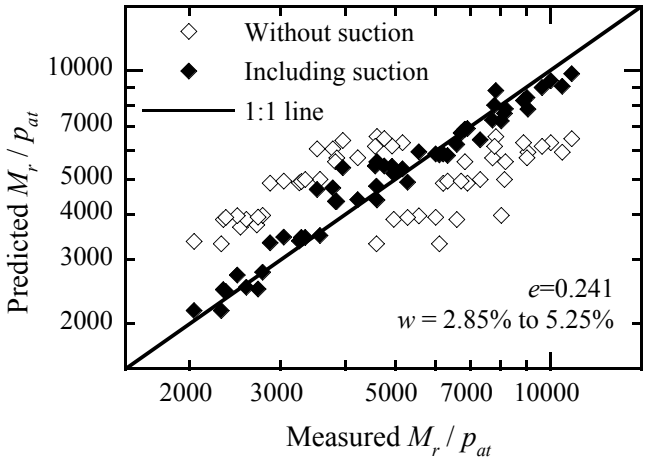

Figure 15: Comparison of measured and predicted resilient modulus

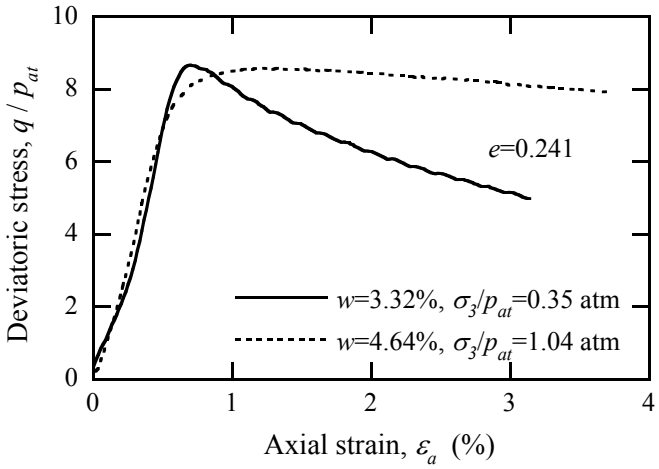

Figure 16: Difference in post peak shear behavior for samples with different w and σ_3